Coastal Engineering 64 (2012) 87–101

Contents lists available at SciVerse ScienceDirect

Coastal Engineering

journal homepage: www.elsevier.com/locate/coastaleng

Probability distribution of individual wave overtopping volumes for smooth impermeable steep slopes with low crest freeboards

L. Victor [a,*], J.W. van der Meer [b], P. Troch [a]

[a] Department of Civil Engineering, Ghent University, Technologiepark 904, B-9052 Zwijnaarde, Belgium
[b] Van der Meer Consulting B.V., P.O. Box 423, 8440 AK, Heerenveen, The Netherlands

ARTICLE INFO

Article history:
Received 7 November 2011
Accepted 16 January 2012
Available online 21 February 2012

Keywords:
Wave overtopping
Individual volumes
Low crest freeboard
Steep slope

ABSTRACT

Several studies showed that the probability distribution of the wave-by-wave (individual) overtopping volumes of traditional sea defense structures is described by a Weibull distribution with a shape factor $b=0.75$. Those structures typically feature relatively large crest freeboards. For the particular design applications of overtopping wave energy converters and smooth dikes in severe storm conditions, knowledge is required on the probability distribution of the individual overtopping volumes of smooth structures with relatively low crest freeboards. This study contributes to a better knowledge on that distribution by analyzing the individual overtopping volumes obtained from new experiments on smooth structures with relatively small crest freeboards ($0.10<R_c/H_{m0}<1.69$) and relatively steep slopes ($0.36<\cot\alpha<2.75$). Furthermore, the characteristics of the corresponding probability distributions are compared to the existing formulations for traditional sea defense structures and submerged dikes or levees. The probability distribution of the individual overtopping volumes for the tested structures also appears to be well described by a Weibull distribution. However, the shape factor b and probability of overtopping P_{ow} (related to the scale factor of the Weibull distribution) are both dependent on the relative crest freeboard and the slope angle. Both b and P_{ow} increase for decreasing relative crest freeboard: b reaches values up to 1.5, while P_{ow} approaches the value of 1.0 (all waves overtop the crest of the structure). Moreover, both the shape factor and probability of overtopping decrease for increasing slope angle. Therefore, two new prediction formulae are proposed for b and P_{ow} based on the new experiments. Finally, based on the relation between the relative 2% run-up height $R_{u2\%}/H_{m0}$ and the probability of overtopping P_{ow}, a new prediction formula for $R_{u2\%}/H_{m0}$ is proposed, bridging the gap between steep slopes and vertical walls adjacent to relatively deep water.

1. Introduction

The crest height design of sea defense structures can be determined by the allowable average overtopping rate $q=[m^3/s/m]$. Extensive research has been carried out in the past on the overtopping behavior of many different types of sea defense structures – smooth dikes, rubble mound structures and vertical walls – resulting in a wide variety of available prediction methods of average overtopping rates q. On the other hand, when considering the effects of wave overtopping on e.g. persons and cars behind the crest of a sea defense structure and on grass erosion resistance, wave-by-wave (individual) volumes V_i [m³/m] and more specific the maximum individual volume V_{max} [m³/m] provide a better design measure than q (Franco et al., 1994). Consequently, the probability distribution of the individual overtopping volumes was studied in the past for sea defense structures, which typically feature high crest freeboards and either mild slopes or vertical walls. Recently, Hughes and Nadal (2009) investigated such probability distribution for dikes with negative crest freeboards. It appears that there is a lack of knowledge on the probability distribution of individual overtopping volumes for structures featuring smooth slopes with low (positive) crest freeboards. Such structures emerge for example in the case of overtopping wave energy converters (Kofoed, 2002) (steep slopes) and in the case of smooth dikes subject to severe storm (design) conditions (milder slopes). The probability distribution of smooth slopes featuring relatively low crest freeboards and relatively steep slopes is studied in the current paper.

The main conclusions of a number of important past studies on the probability distribution of individual overtopping volumes for coastal structures are presented and discussed in Section 2. The study in current paper is based on an analysis of the probability distribution of the individual overtopping volumes for smooth impermeable steep slopes with low crest freeboards, measured during new experiments. The test set-up and test matrix of the new experiments are described in Section 3. The test results of the new experiments for the probability distribution of the individual volumes are shown and compared

* Corresponding author. Tel.: +32 9 264 55 71; fax: +32 9 264 58 37.
E-mail addresses: lander.victor@ugent.be (L. Victor), peter.troch@ugent.be (P. Troch).

0378-3839/$ – see front matter © 2012 Elsevier B.V. All rights reserved.
doi:10.1016/j.coastaleng.2012.01.003

to existing formulations for coastal structures (Section 2) in Sections 4 and 5. The shape of the distribution is discussed in Section 4, while the overtopping probability – which is an important parameter for the scale of the distribution – is treated in Section 5.

2. Existing formulations for probability distribution of individual overtopping volumes

2.1. Probability distribution of individual overtopping volumes for sea defense structures

One of the first studies on the probability distribution of individual overtopping volumes for coastal structures was made by Van der Meer and Janssen (1994) based on an investigation on wave overtopping at sloped coastal structures. The conclusion was drawn that the exceedance probability of each overtopping volume P_V [−] (related to the number of overtopping waves N_{ow} [−]) is well fitted by a two-parameter Weibull distribution function:

$$P_V = P[V_i \geq V] = \exp\left(-\left(\frac{V}{a}\right)^b\right). \quad (1)$$

The coefficient b [−] determines the shape of the distribution and is therefore referred to as the shape factor. The shape factor b was assigned a constant value of 0.75 for sloped coastal structures by Van der Meer and Janssen (1994). The corresponding value of the scale factor a [m³/m] is equal to:

$$a = 0.84\frac{q\,N_w T_m}{N_{ow}} = 0.84\frac{qT_m}{P_{ow}}. \quad (2)$$

T_m [s] is the average wave period, while P_{ow} is the probability of wave overtopping is defined by Eq. (3), i.e. the proportion of the number of overtopping waves N_{ow} and the number of waves N_w [−].

$$P_{ow} = \frac{N_{ow}}{N_w}. \quad (3)$$

Identical formulations for a and b were used by TAW (2002) and more recently by the Overtopping Manual (EurOtop, 2007).

Eq. (2), found by Van der Meer and Janssen (1994) is mathematically derived below. The derivation starts from the definition of the average overtopping rate q as the proportion of the total overtopping volume V_0 [m³/m], i.e. the sum of individual volumes V_i, and the sum T_0 [s] of the wave periods of each wave in the wave train T_i [s]:

$$q = \frac{V_0}{T_0} = \frac{\sum V_i}{\sum T_i} = \frac{\sum V_i}{N_w T_m} \quad (4)$$

$$\Rightarrow \frac{q\,N_w T_m}{N_{ow}} = \frac{\sum V_i}{N_{ow}}. \quad (5)$$

The right hand side of Eq. (5) equals the measured mean overtopping volume, denoted by $\bar{V}_{meas}$ [m³/m]:

$$\bar{V}_{meas} = \frac{\sum V_i}{N_{ow}} = \frac{V_0}{N_{ow}}. \quad (6)$$

Based on the definition of a two-parameter Weibull (Eq. (1)), the theoretical average overtopping volume is expressed by:

$$\bar{V}_{theor} = E[V]_{Weibull} = a\Gamma\left(1+\frac{1}{b}\right). \quad (7)$$

Γ stands for the mathematical gamma function, for which values are available in tabled form in literature. When the two-parameter Weibull distribution properly characterizes the individual overtopping volumes, the expressions for $\bar{V}_{meas}$ (Eq. (6)) and $\bar{V}_{theor}$ (Eq. (7)) are equal to each other. Accordingly, the following relationship exists between a and b:

$$a = \frac{1}{\Gamma\left(1+\frac{1}{b}\right)}\,\frac{qN_w T_m}{N_{ow}}. \quad (8)$$

The coefficient a is proportional to the average overtopping volume, consequently scaling the individual volumes in Eq. (1). This explains the name scale factor of the coefficient a. Larger values of V_i correspond to larger values of the scale factor a.

The coefficient $1/\Gamma\left(1+\frac{1}{b}\right)$ in Eq. (8) is referred to as a' [−]. Values of a' are given in Table 1 for a shape factor b ranging from 0.60 to 2.0; a graphical representation is shown in Fig. 1. The value of b is expected to be within this range of b-values for structures with a positive crest freeboard (see e.g. Besley, 1999). The upper boundary ($b=2.0$) corresponds to a Rayleigh distribution.

The relationship between the coefficient a' and the shape factor b is accurately expressed using a hyperbolic tangent fit (Eq. (9)) for the range of application of b in Table 1 and Fig. 1 (the corresponding value of the determination coefficient r^2 is 0.96).

$$a' = 1.13\tanh(1.132b). \quad (9)$$

The value of a' corresponding to $b=0.75$ equals 0.84 (Eq. (2)). For values of $1.5 \leq b \geq 2.0$, a' reaches a maximum of approximately 1.13.

A more detailed analysis of the shape factor b has been carried out by Besley (1999) based on a number of datasets restricted to more limited types of sea defense structures. The applicability of the two-parameter Weibull distribution for sea defense structures has been confirmed for all tested structures. Furthermore, Besley (1999) did not focus on an "average" value of the shape factor b, but fitted values of b to each dataset. The shape factor appears to be dependent on the wave steepness $s_p = 2\pi H_s/(gT_p^2)$ [−] and on the occurrence of impacting waves (Table 2). A dependency on the slope angle a' has also been noticed by Besley (1999). However, no distinct pattern has been recognized for the effect of the slope angle on b. Hence, its effect is not present in Table 2. The values of the scale factor corresponding to the shape factors in Table 2 are calculated based on Eq. (8).

The more detailed analysis by Besley (1999) results in values of the shape factor b for smooth sloping structures and vertical walls subjected to non-impacting waves that are mostly within the range $0.60 \leq b \leq 0.90$. Since the average value $b=0.75$ of this interval is identical to the shape factor derived by Van der Meer and Janssen (1994) and Franco et al. (1994), one may question the usefulness of using different shape factors over the constant value 0.75. Therefore, a shape factor $b=0.75$ is normally applied for smooth structures, which means that the effect of the wave steepness and the type of smooth structure (either sloping or vertical) are neglected.

Table 1
a' as a function of the shape factor b for a two-parameter Weibull distribution, with b ranging between 0.60 and 2.0.

Shape factor b [−]	Coefficient a'
0.60	0.66
0.75	0.84
0.90	0.95
1.05	1.02
1.20	1.06
1.35	1.09
1.50	1.11
1.65	1.12
1.80	1.12
1.95	1.13
2.00	1.13

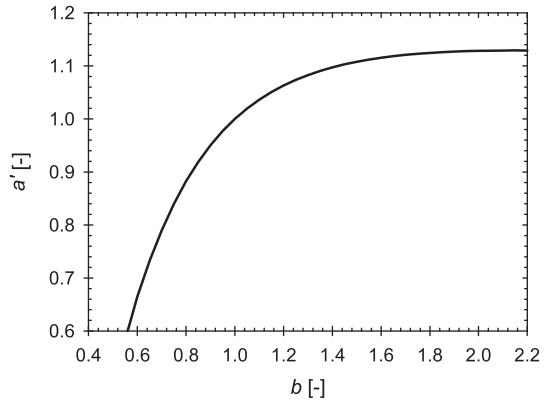

Fig. 1. Coefficient a' as a function of the shape factor b for a two-parameter Weibull distribution, with b ranging between 0.60 and 2.0.

Bruce et al. (2009) concluded that the effect of the wave steepness on the shape of the Weibull distribution is unclear for rubble mound breakwaters, based on a large dataset of experiments with those structures. A detailed analysis showed that the shape factor of the distribution is most accurately represented by its average value: $b=0.74$. Hence, the test results for rubble mound breakwaters also provided little support to change the generally applicable shape factor $b=0.75$.

In conclusion, the average value of the shape factor b is approximately 0.75 for the different types of sea defense structures (sloped smooth, vertical and rubble mound breakwaters). The corresponding probability distribution is determined by Eqs. (1) and (2). Only the probability of overtopping P_{ow} is unknown in Eq. (2). A number of expressions for P_{ow} are available in literature, as discussed in the next Section 2.2.

2.2. Probability of overtopping P_{ow} for sea defense structures

Van der Meer and Janssen (1994) and Franco et al. (1994) assumed the run-up heights of the considered structures are Rayleigh distributed and gave the following expression for the probability of overtopping P_{ow}:

$$P_{ow} = \exp\left(-\left(\frac{1}{\chi}\frac{R_c}{H_{mo}}\right)^2\right). \tag{10}$$

The value of the coefficient χ [−] in Eq. (10) is related to the relative 2% run-up height $R_{u2\%}/H_{mo}$ [−]:

$$\chi = \frac{R_{u2\%}}{H_{mo}}\frac{1}{\sqrt{-\ln(0.02)}} \approx 0.51\frac{R_{u2\%}}{H_{mo}}. \tag{11}$$

Van der Meer and Janssen (1994) derived the following well-validated expression for the relative 2% run-up height of sloping smooth structures:

$$\frac{R_{u2\%}}{H_{mo}} = 1.5\gamma_h\gamma_f\gamma_\beta\gamma_b\xi_p \tag{12a}$$

Table 2
Shape factor b by Besley (1999).

	$s_p=0.02$	$s_p=0.04$
Vertical wall, non-impacting waves	0.66	0.82
Vertical, impacting waves	0.85	0.85
Smooth sloping structures	0.76	0.92

for breaking waves, with a maximum for non-breaking waves of:

$$\frac{R_{u2\%}}{H_{mo}} = 3.0\gamma_h\gamma_f\gamma_\beta. \tag{12b}$$

The breaker parameter ξ_p [−] is defined by $\tan\alpha/\sqrt{s_p}$. The corresponding expressions for the coefficient χ are:

$$\chi = 0.76\gamma_h\gamma_f\gamma_\beta\gamma_b\xi_p \tag{13a}$$

with a maximum of:

$$\chi = 1.52\gamma_h\gamma_f\gamma_\beta. \tag{13b}$$

The γ-factors are influence or reduction factors which take into account the effects of a shallow foreshore (γ_h), the slope roughness (γ_f), oblique wave attack (γ_β) and a berm (γ_b). Eqs. (13a)–(13b) gives the mean of a stochastic parameter with variation coefficient $\sigma/\mu=0.06$.

Based on a larger number of experimental datasets with sloped coastal structures, TAW (2002) derived a slightly different expression for the relative 2% run-up height with the breaker parameter based on the mean spectral wave period Tm-1,0 [s]:

$$\frac{R_{u2\%}}{H_{mo}} = 1.65\gamma_h\gamma_f\gamma_\beta\gamma_b\xi_{m-1,0} \tag{14a}$$

with a maximum of:

$$\frac{R_{u2\%}}{H_{mo}} = 1.0\gamma_f\gamma_\beta\gamma_b\left(4.0-\frac{1.5}{\sqrt{\xi_{m-1,0}}}\right). \tag{14b}$$

The range of application of Eqs. (14a)–(14b) for $\gamma_b\xi_{m-1,0}$ is: $0.5<\gamma_b\xi_{m-1,0}<8.0$ to 10.0. The reliability of Eqs. (14a)–(14b) is expressed by considering Eqs. (14a)–(14b) as the mean of a stochastic parameter $R_{u2\%}/H_{mo}$ with variation coefficient $\sigma/\mu=0.07$. In contrast to the constant maximum relative 2% run-up height for non-breaking waves in Eq. (13b), a continuously increasing relative 2% run-up height is predicted by Eq. (14b) for large values of the breaker parameter.

The formulations by (TAW, 2002) are inserted in the Overtopping Manual, (EurOtop, 2007).

Instead of using an expression for $R_{u2\%}/H_{mo}$ of vertical walls, Franco et al. (1994) used a best fit of their experimental test results for vertical walls in relatively deep water to Eq. (10), resulting in a coefficient $\chi=0.91$.

2.3. Probability distribution of individual overtopping volumes for negative crest freeboards

Hughes and Nadal (2009) investigated the probability distribution of individual overtopping volumes for levees or dikes subjected to combined wave overtopping and storm surge overflow. Accordingly, the tested structures featured negative crest freeboards, with $-2.0<R_c/H_{mo}<0.0$. The overtopping probability P_{ow} is 1.0.

Individual overtopping volumes have been identified based on the time series of the water depth measured at a location on the crest of the tested structures. The distribution of the individual overtopping volumes still fits the two-parameter Weibull distribution (Eq. (1)), with values of the shape factor b ranging between 1.0 and 3.5 for the 27 tests carried out by Hughes and Nadal (2009). The values diverge strongly from the shape factor $b=0.75$, but submerged levees or dikes are also very different from emerged dikes.

The measured average overtopping rate q_{ws} consists of both a component related to wave overtopping (q_w) and a component due to surge overflow (q_s). Hence, Eq. (4) is no longer valid. Furthermore, the relationship between the scale factor a and shape factor b

established in Eq. (8) is only valid when the scale factor is determined based on the component of the average overtopping rate due to wave overtopping q_w. However, since only the total average overtopping rate q_{ws} was measured, Eq. (8) is not applicable. Instead, two independent expressions for the shape factor (Eq. (15)) and scale factor (Eq. (16)) were derived.

$$a = 0.79\, q_{ws} T_p \tag{15}$$

$$b = 15.7\left(\frac{q_s}{gT_p H_{mo}}\right)^{0.35} - 2.3\left(\frac{q_s}{\sqrt{gH_{m0}^3}}\right)^{0.79}. \tag{16}$$

Note that Eq. (15) resembles Eq. (2) relatively well, taking into account the value of the overtopping probability $P_{ow} = 1.0$. Only the characteristic wave period is different. This confirms the validity of Eq. (15).

3. Applicability of existing formulations to steep low-crested slopes

3.1. General

The existing formulations for the probability distribution of the individual overtopping volumes (Section 2) mainly apply to the neighboring structures (from a geometrical point of view) of the steep low-crested slopes with positive crest freeboard considered in this paper. Correspondingly, these formulations allow to draw a number of conclusions concerning the probability distribution of the individual overtopping volumes of steep low-crested slopes.

First, the probability distribution is expected to be well described by a two-parameter Weibull distribution (Eq. (1)). Furthermore, since the structures feature positive crest freeboards, no surge overflow occurs. This means Eq. (4) is still valid. The expected values for the shape factor b and for the probability of overtopping b are discussed in Sections 3.2 and 3.3 respectively.

3.2. Shape factor b

Based on the existing formulations, the following conclusions are drawn concerning the value of the shape factor of the Weibull distribution for steep low-crested slopes:

- both for vertical walls and mildly sloping dikes with relatively high crest freeboards, the value of the shape factor b is approximately 0.75. Since the effect of the slope angle on b is unclear (Besley, 1999), the shape factor for steep slopes with relatively high crest freeboard is expected to be $b = 0.75$ as well;
- on the other hand, since structures with negative crest freeboards correspond to values of the shape factor larger than 1.0, the shape factors for the structures with relatively low relative crest freeboards are expected to be larger than 0.75.

These conclusions point at a dependency of the shape factor on the relative crest freeboard. In order to show the effect of a shape factor larger than 0.75 on the probability distribution of the individual overtopping volumes, four examples of a theoretical two-parameter Weibull distribution are given in Fig. 2: with shape factor $b = 0.75$ (dash-dotted line), $b = 1.0$ (dotted line), $b = 2.0$ (short-dashed line) and $b = 3.0$ (long-dashed line).

The dotted line corresponds to the exponential curve. The short-dashed line shows the Rayleigh distribution (i.e. the distribution of the wave heights in deep water) which is a straight line in Fig. 2 since the horizontal axis is scaled according to a Rayleigh distribution. The theoretical distribution with $b = 3.0$ is also shown in Fig. 2; this is a value of the shape factor found by Hughes and Nadal (2009) for negative crest freeboards.

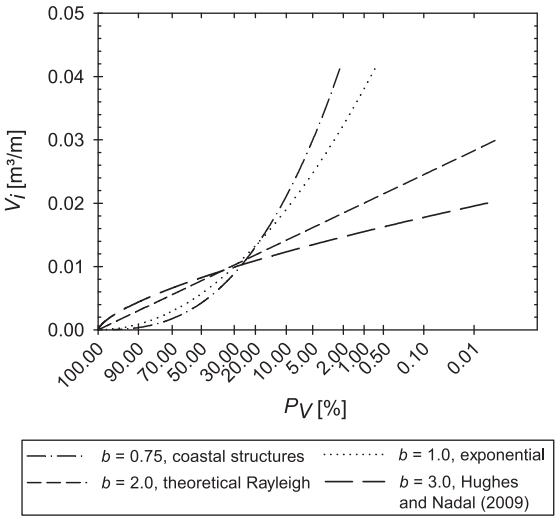

Fig. 2. Theoretical probability distributions of individual wave overtopping volumes for $\bar{V}_{meas} = 0.008$ m³/m with b = 0.75, 1.0, 2.0 and 3.0.

When $b = 0.75$, large part of the overtopping volumes are relatively small, while only a small percentage of the volumes is very large (EurOtop, 2007). Such distribution is typical for sea defense structures, for which the average overtopping rate is largely determined by a small number of very large overtopping volumes (EurOtop, 2007).

On the other hand, the overtopping volumes are more evenly distributed when b becomes larger: a larger percentage of overtopping volumes contributes considerably to the average overtopping rate. Since the values of the shape factor found by Hughes and Nadal (2009) are of the order of 2.0 and 3.0, a more even distribution of the overtopping volumes applies for structures with a negative crest freeboard.

Furthermore, a small value of the shape factor corresponds to larger maximum volumes. This means that the value of the shape factor is important for the design of sea defense structures. Applying a smaller shape factor results in a more conservative approach For example, an overprediction of the largest overtopping volumes corresponds to flow velocities that are too large. This results in overly safe dimensions of slope protections and crest freeboards.

3.3. Probability of overtopping a_{coeff}

The probability of overtopping P_{ow} for sloping structures is traditionally related to the relative crest freeboard and the relative 2% run-up height, determined for non-overtopped structures (Section 2.2).

The commonly used formula for the relative 2% run-up height $R_{u2\%}/H_{m0}$ in Eqs. (14a)–(14b) predicts a continuous increase in relative 2% run-up height for increasing value of the breaker parameter (Fig. 3). However, this equation has been derived from tests by Van Gent (2001) on dikes with shallow foreshores, resulting in small values of the wave steepness and thus large breaker parameters, not on tests with steep slopes. When the large breaker parameters are due to steep slopes, the value of $R_{u2\%}/H_{m0}$ is expected to decrease towards the theoretical value for vertical walls (dotted line in Fig. 3) which is positioned significantly below the predictions by Eqs. (14a)–(14b). The dotted line is also positioned significantly below the prediction line of Eqs. (13a)–(13b).

The theoretical relative 2% run-up height for vertical walls in Fig. 3 is determined as follows. Wave reflection at non-overtopped vertical walls is presumed to be 100%. Accordingly, the theoretical run-up height for a wave at a vertical non-overtopped wall is equal to its wave height. Hence, the run-up height distribution follows the

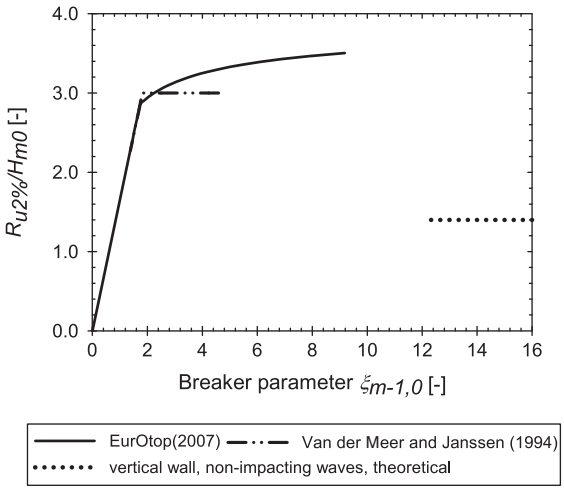

Fig. 3. Predicted relative 2% run-up height as a function of the breaker parameter for a wave height $H_{m0}=0.100$ m and a wave period $T_p=1.534$ s.

wave height distribution. Assuming that the wave heights follow a Rayleigh distribution, a fixed relationship exists between $R_{u2\%}$ and H_{m0}:

$$\frac{R_{u2\%}}{H_{m0}}=\frac{H_{2\%}}{H_{m0}}=1.4. \tag{17}$$

Based on Eq. (11) and the value $\chi=0.91$ found by Franco et al. (1994) for vertical walls in relatively deep water, the relative 2% run-up height for those vertical walls is approximately 1.8. This value is slightly larger than the theoretical value in Eq. (17).

In conclusion, a decrease in $R_{u2\%}/H_{m0}$ is expected to occur for steep slopes toward the theoretical value for vertical walls (Eq. (17)).

Both the value of the shape factor b and the expression of the probability of overtopping P_{ow} require further investigation for steep low-crested slopes. This investigation has been carried out based on the UG10 test series. A description of these test series is given in the next section.

4. Description of the test set-up and test matrix of the new experiments

The new experiments were carried out at the Department of Civil Engineering at Ghent University (Belgium) in a wave flume with dimensions 30 m × 1 m × 1.2 m (length × width × height), which is equipped with a piston-type wave generator. The tested structures feature smooth impermeable steep slopes extending to the seabed and low crest freeboards. The amount of overtopped water was determined using the weigh cell technique (e.g. Franco et al., 1994; Schüttrumpf, 2001). The test set-up of the new experiments is particularly designed to measure large wave-by-wave overtopping volumes accurately. A definition sketch of the test set-up is shown in Fig. 4.

In order to study the independent effects of the relative crest freeboard R_c/H_{m0}, slope angle α and wave steepness $s_{m-1,0}$ on the probability distribution of the individual overtopping volumes, broad ranges of those three parameters were used during the experiments.

A varying crest freeboard was achieved by changing the water depth h_t between 0.50 m, 0.53 m and 0.55 m. The corresponding values for the crest freeboard R_c are 0.07 m, 0.05 m and 0.02 m respectively. The slope angle of the tested structures was varied between $\cot\alpha = 0.36$ (70°) and $\cot\alpha = 2.75$ (20°) (nine slopes). Each of the slope angles is combined with three crest freeboards.

The different geometries have been subjected to irregular waves, generated using a piston-type wave paddle. A summary of the combinations of spectral significant wave height H_{m0} and peak period T_p during the UG10 test series is shown in Table 3. A parameterized JONSWAP spectrum with peak enhancement factor 3.3 is applied. At least 1000 waves have been generated for each experimental test, in order to obtain values of the average overtopping rate that are statistically independent of the number of waves of the test.

In total, 364 irregular wave tests have been carried out. The results are gathered in a dataset referred to as the UG10 dataset. The corresponding ranges of application for the relative crest freeboard R_c/H_{m0}, slope angle α and wave steepness $s_{m-1,0}$ are: $0.10\le R_c/H_{m0}\le 1.69$, $\cot\alpha\in[0.36, 0.58, 0.84, 1.00, 1.19, 1.43, 1.73, 2.14, 2.75]$ and $0.02\le s_{m-1,0}\le 0.05$. The ranges partly overlap those for sea defense structures, allowing a validation of the new test results against existing knowledge for sea defense structures. Due to the steep slopes, the major part of the new test results corresponds to non-breaking waves (i.e. approximately for $\xi_{m-1,0}>2.0$ (EurOtop, 2007)) on the slope of the structure: $2.0<\xi_{m-1,0}>21.5$.

It should be noted that the wave heights of the new experimental tests with large significant wave heights H_{m0} did not fit a Rayleigh distribution, but a composite Weibull distribution described by Battjes and Groenendijk (2000). This composite Weibull distribution features lower probabilities of occurrence for the largest wave heights compared to a Rayleigh distribution. Consequently, the deviations from the Rayleigh distribution are caused by depth induced breaking of the largest waves in the wave trains for the new experimental tests with large significant wave heights.

5. Probability distribution of individual overtopping volumes for UG10 test series

Individual overtopping volumes have been determined accurately for each test of the UG10 test series based on the weigh cell signal. Successively, a Weibull plot has been generated for each test of the UG10 test series (1) in order to verify if these volumes follow a two-parameter Weibull distribution, and (2) to determine the scale factor a and shape factor b of that Weibull distribution. This methodology was also applied when deriving the expressions of the

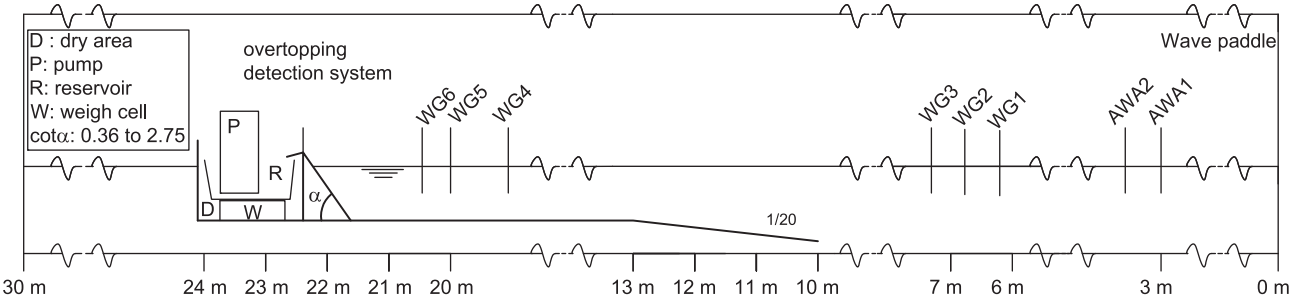

Fig. 4. Definition sketch of the test set-up of the new experiments. A cross-section along the length of the flume is shown. WG stands for wave gage, AWA stands for wave gage used for active wave absorption.

Table 3
Test matrix of UG10 test series.

9 slope angles						
	3 crest freeboards					
	H_s [m]	T_p [s]				
		1.022	1.278	1.534	1.789	2.045
	0.020	W01				
	0.033	W11	W12			
	0.067	W21	W22	W23		
	0.100		W32	W33	W34	
	0.133			W43	W44	W45
	0.167				W54	W55
	0.185					W65

probability distribution for the traditional sea defense structures in Section 2.1. The principle of a Weibull plot is explained in the following Section 5.1.

5.1. Weibull plot for UG10 tests

The method to generate a Weibull plot is explained hereafter. It is based on Eq. (18). Based on Eq. (1), the following expression is found for the individual overtopping volume:

$$V = a(-(\ln P_v))^{\frac{1}{b}}. \tag{18}$$

By taking the logarithm of its both sides, Eq. (18) is converted into:

$$\log V = \log a + \frac{1}{b}\log(-\ln y). \tag{19}$$

The theoretical exceedance probability P_V is approximated by the empirical exceedance probability $\hat{P}_V$ (Eq. (20)), denoted by y.

$$\hat{P}_V = y = \frac{m}{N+1}. \tag{20}$$

By setting $\log a = \lambda$ and $1/b = \psi$, Eq. (19) can be rewritten as:

$$\log V = \lambda + \psi \log(-\ln y). \tag{21}$$

Eq. (21) is the basic equation for the Weibull plot, which consists of a plot of $\log V$ for all measured individual overtopping volumes as a function of $\log(-\ln y)$. When the data points follow a linear trend in the Weibull plot, the distribution of the individual overtopping volumes fits a two-parameter Weibull distribution. Based on Eq. (21), the scale factor a is related to the intersection point of the linear trend line with the vertical axis of the Weibull plot, while the shape factor b is linked to the slope angle of that trend line.

An example of a Weibull plot is given in Fig. 5 (low probability of exceedance is to the right of Fig. 5) for a test of the UG10 dataset with $H_{m0} = 0.10$ m, $R_c = 0.02$ m, T_p 1.79 s and $\cot\alpha = 1.0$. The corresponding relative crest freeboard is $R_c/H_{m0} = 0.20$. The general trend described by the data points in Fig. 5 is linear, and the conclusion is drawn that the individual volumes fit a two-parameter Weibull distribution. The data points corresponding to the example in Fig. 5 are also plotted in a graph similar to Fig. 2 (Fig. 6), with a Rayleigh scale on the horizontal axis.

The small overtopping volumes deviate most significantly from the linear trend and affect the slope angle of the corresponding linear trend line to a large extent. On the other hand, Fig. 6 shows that the contribution of the small volumes to the probability distribution is actually rather limited. Accordingly, the characteristics of the Weibull plot have been determined without considering the small overtopping volumes.

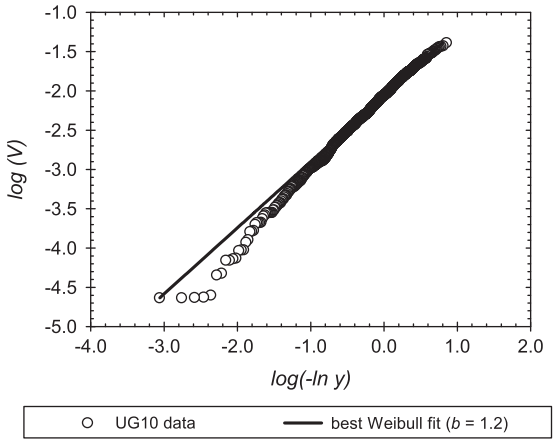

Fig. 5. Weibull plot for a test of the UG10 dataset with $H_{m0} = 0.100$ m, $R_c = 0.020$ m, $T_p = 1.789$ s and $\cot\alpha = 1.0$. The corresponding relative crest freeboard is $R_c/H_{m0} = 0.20$.

It has been emphasized by Van der Meer and Janssen (1994) and Besley (1999) that the two-parameter Weibull distribution is particularly a good fit at higher values of the individual volumes and thus is able to accurately represent extreme values of V_i, both for sloped sea defense structures and vertical walls. Hence, the coefficients a and b are traditionally determined by only considering a particular percentage of the largest individual volumes. For example, the Weibull distribution is only fitted to individual volumes $V_i > \bar{V}_{meas}$ for smooth dikes by Van der Meer and Janssen (1994) and for vertical walls studied by Besley et al. (1998), since this gave the most reliable estimates of V_{max}. An identical approach has been applied by Bruce et al. (2009) for rubble mound breakwaters.

On the other hand, when studying the distribution of individual volumes for the optimization of OWECs, all volumes should be considered since the design of the reservoir and turbines is based on realistic simulations of individual wave overtopping volumes and not on the maximum volume. However, the small volumes should also be left out of the linear regression analysis for OWECs, since these volumes distort the slope angle of the linear trend line in the Weibull plot.

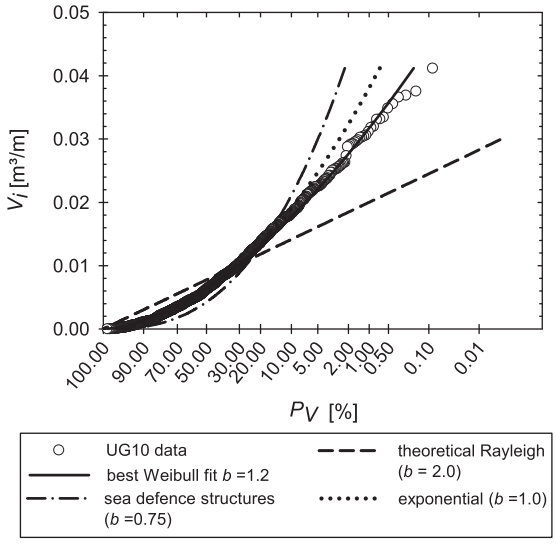

Fig. 6. Individual overtopping volume V_i against the exceedance probability P_V for a test of the UG10 dataset with $H_{m0} = 0.100$ m, $R_c = 0.020$ m, $T_p = 1.789$ s and $\cot\alpha = 1.0$ with its best Weibull fit. The theoretical two-parameter Weibull distributions with $b = 0.75$, $b = 1.0$ and $b = 2.0$ are added. The horizontal axis is scaled according to a Rayleigh distribution.

Furthermore, a constraint on the possible combinations of a and b is established by the relationship between a and b in Eq. (8). For large values of b (but smaller than 2.0) the value of a' is approximately constant (Fig. 1). This means that the intersection point of the linear trend line of the data points with the vertical axis of the Weibull plot is approximately constant for large values of b of say $1.5<b<2.0$.

Eventually, the coefficients a and b have been determined for the tests of the UG10 test series based on a Weibull plot of the individual overtopping volumes with $V_i > \bar{V}_{meas}$. The corresponding Weibull distributions are referred to as the best Weibull fits. A best Weibull fit has been determined for each test of the UG10 dataset.

The shape factor for the example shown in Fig. 5, only taking into account the individual volumes $V_i > \bar{V}_{meas}$, equals $b=1.2$. The best Weibull fit for that particular example is added to Figs. 5 and 6. Based on Fig. 6, this fit is positioned in between the long-dashed line corresponding to the two-parameter Weibull distribution for sea defense structures ($b=0.75$) and the short-dashed line of the theoretical Rayleigh distribution ($b=2.0$), close to an exponential distribution.

5.2. Effect of non-Rayleigh distributed wave heights on shape factor b

Among the 364 UG10 tests considered for studying the probability distribution of steep low-crested slopes, a number of tests correspond to non-Rayleigh distributed wave heights (Section 4). Although the sea state is categorized as non-breaking, depth-induced breaking of the largest waves occurs, limiting the value of the maximum individual volume. In accordance to Fig. 2, a decrease in the largest individual volumes corresponds to an increase in the value of the shape factor b.

The differences in the Weibull distribution between a test with Rayleigh distributed wave heights and a test with non-Rayleigh distributed wave heights are clear when comparing Figs. 5 and 7 on the one hand, and Figs. 6 and 8 on the other hand. Although both tests correspond to identical slope angles and a similar value of the relative crest freeboard, the shape factor in Figs. 5 and 6 is 1.2, while it is 1.4 for the case shown in Figs. 7 and 8. The probability distribution in Fig. 8 is a little flatter, due to the non-Rayleigh distribution of the wave heights. The linear trend line of the largest volumes clearly deviates from the linear trend line followed by the medium-sized overtopping volumes. Furthermore, the smallest individual volumes are not accurately described by the Weibull distribution derived based on the individual overtopping volumes V_i larger than $\bar{V}_{meas}$ (Fig. 8).

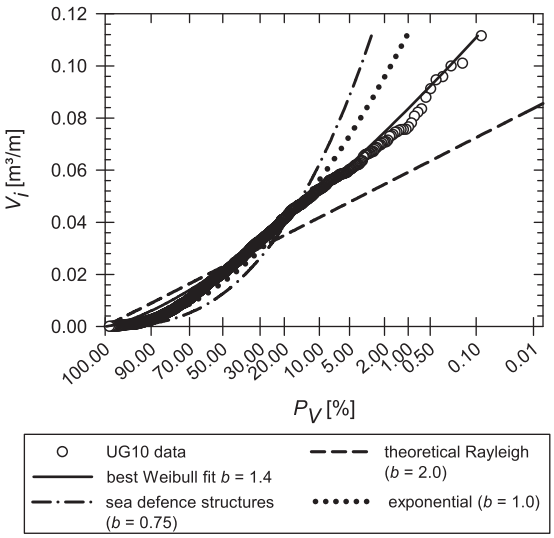

Fig. 8. Graph of individual overtopping volume V_i against the exceedance probability P_V for a test of the UG10 dataset with $H_{m0}=0.185$ m, $R_c=0.045$ m, $T_p=2.045$ s and $\cot\alpha=0.58$ with its best Weibull fit. The theoretical two-parameter Weibull distributions with $b=0.75$, $b=1.0$ and $b=2.0$ are added. The horizontal axis is scaled according to a Rayleigh distribution.

The example in Figs. 7 and 8 shows that when the wave heights are not Rayleigh distributed, the distribution of the individual overtopping volumes is more accurately described by using two Weibull distributions, similar to the distribution of the wave heights (Battjes and Groenendijk, 2000).

The differences in the wave height distribution between the UG10 tests in Figs. 6 and 8 are explicitly shown in Figs. 9 and 10. The wave heights in Fig. 9 (corresponding to the example in Fig. 6) clearly follow the Rayleigh distribution, while the wave heights in Fig. 10 (corresponding to the example in Fig. 8) clearly deviate from the Rayleigh distribution.

The observation that tests with non-Rayleigh distributed wave heights corresponds to larger values of the shape factor b should be kept in mind when studying the effects of the slope angle, relative crest freeboard and wave steepness on the shape factor b of the Weibull distribution of the individual overtopping volumes for steep low-crested slopes. These effects have been studied based on the best Weibull fits for the 364 tests of the UG10 test series, as discussed in the following three Sections 5.3 to 5.5.

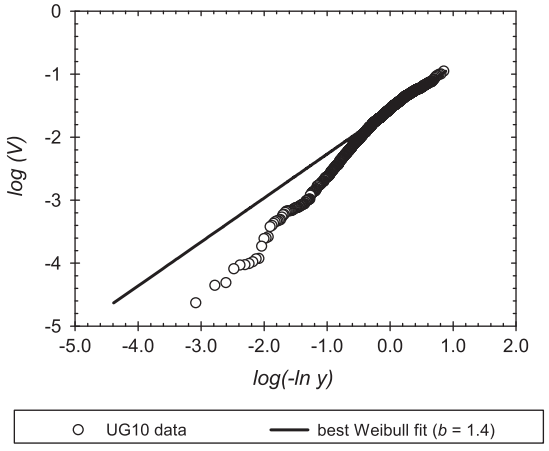

Fig. 7. Weibull plot for UG10 test results with $H_{m0}=0.1185$ m, $R_c=0.045$ m, $T_p=2.045$ s and $\cot\alpha=1.0$. The corresponding relative crest freeboard is $R_c/H_{m0}=0.24$.

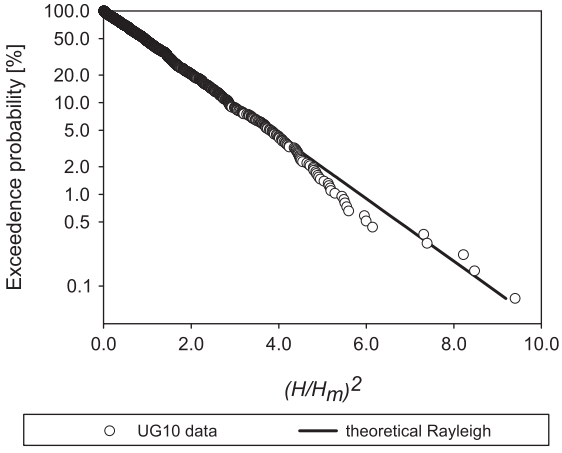

Fig. 9. Probability distribution of individual wave heights for UG10 test with $H_{m0}=0.10$ m, $R_c=0.020$ m, $T_p=1.789$ s and $\cot\alpha=1.0$. The corresponding relative crest freeboard is $R_c/H_{m0}=0.20$.

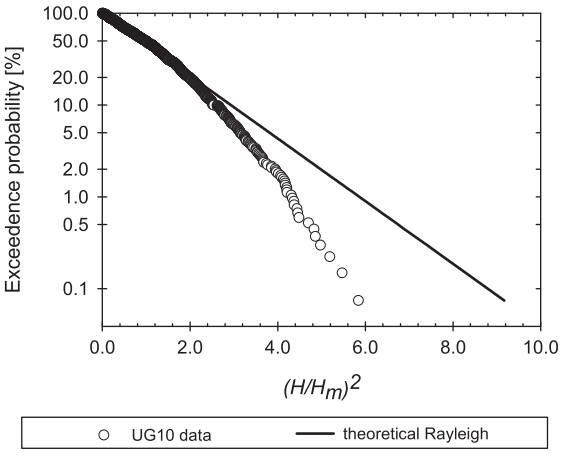

Fig. 10. Probability distribution of individual wave heights for UG10 test results with $H_{m0}=0.185$ m, $R_c=0.045$ m, $T_p=2.045$ s and cot $\alpha=1.0$. The corresponding relative crest freeboard is $R_c/H_{m0}=0.24$.

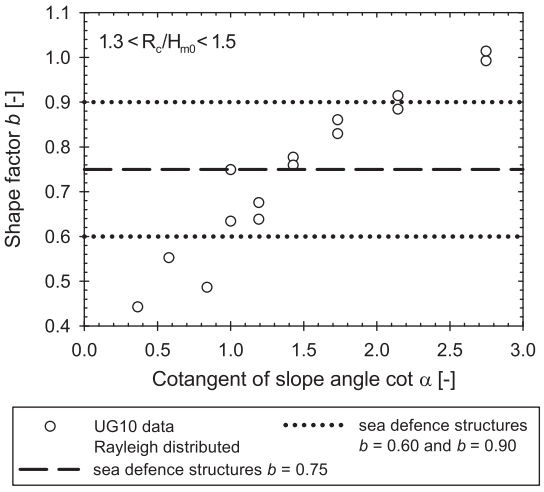

Fig. 12. Effect of slope angle on the shape factor b for $1.3<R_c/H_{m0}<1.5$.

5.3. Effect of slope angle on shape factor b

A clear effect of the slope angle on the shape factor b is distinguished for the test results of the UG10 dataset with $0.8<R_c/H_{m0}<1.0$ which corresponds to Rayleigh distributed wave heights at the toe of the structure (Fig. 11). The shape factor increases from 0.8 for cot $\alpha=0.36$ to 1.07 for cot $\alpha=2.75$, approximately following a linear trend line.

Based on similar graphs for other ranges of R_c/H_{m0} (e.g. Figs. 12 and 13), it appears that the dependency of the shape factor on the slope angle for steep low-crested slopes in general follows a linear trend line, increasing for decreasing slope angle. Fig. 12 shows the effect of the slope angle on the shape factor of the Weibull distribution for relatively large crest freeboards. The linear increasing trend is clearly visible. This is in contrast to the findings by Besley (1999) that a clear effect of the slope angle on the shape factor b could not be distinguished for sea defense structures. On the other hand, the average value of the shape factor in Fig. 12 is still equal to 0.75, i.e. the value traditionally used for sea defense structures (Section 2.1).

The general conclusion of the linear trend line is also valid for tests of the UG10 test series with non-Rayleigh distributed wave heights (marked in black in Fig. 13). The corresponding shape factors are larger than the shape factors for the tests with Rayleigh distributed wave heights (see Section 5.2).

Approximately all data points in Fig. 13 correspond to a shape factor larger than 1.0. This is due to the relatively small crest freeboards of those data points. The effect of the relative crest freeboard on the shape factor b is discussed in the next Section 5.4.

5.4. Effect of relative crest freeboard on shape factor b

The effect of the relative crest freeboard on the shape factor b for the UG10 test results with Rayleigh distributed wave heights is shown in Fig. 14. For a particular slope angle, an increase in relative crest freeboard causes a decrease of the shape factor b, until it approximately reaches a constant for $R_c/H_{m0}>1.2$. The data points approximately follow a negative exponential trend line for each value of the slope angle α.

The data points corresponding to tests with $R_c/H_{m0}>1.2$ are in general positioned around the shape factor $b=0.75$, confirming the validity of the predicted characteristics for the Weibull distribution of sea defense structures (Section 2.1) for steep slopes with relatively large crest freeboards (see also discussion on Fig. 12 in Section 5.3).

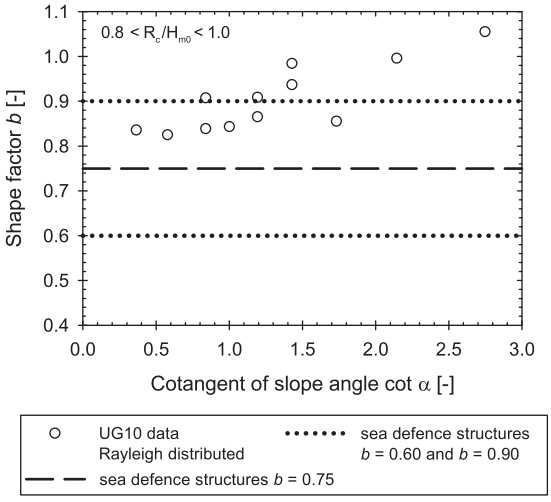

Fig. 11. Effect of the slope angle on the shape factor b for $0.8<R_c/H_{m0}<1.0$.

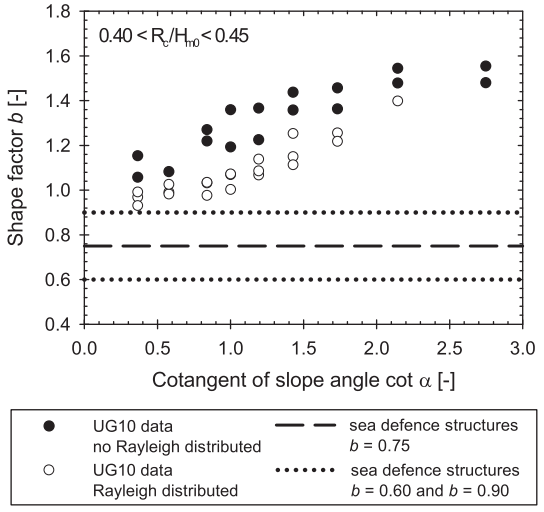

Fig. 13. Effect of slope angle on the shape factor b for $0.40<R_c/H_{m0}<0.45$.

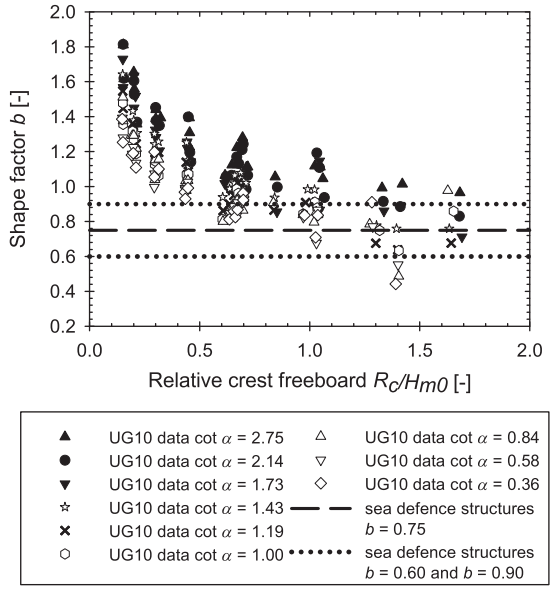

Fig. 14. Effect of the relative crest freeboard on the shape factor b, for UG10 test results with Rayleigh distributed wave heights.

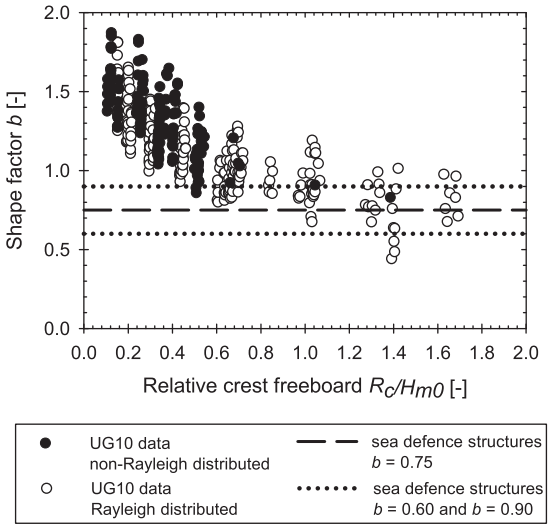

Fig. 16. Effect of the relative crest freeboard on the shape factor b, for UG10 test results with Rayleigh distributed wave height and non-Rayleigh distributed wave heights.

On the other hand, the majority of the data points with $R_c/H_{m0} > 1.2$ are positioned above the horizontal line corresponding to $b = 0.75$. Furthermore, the deviation increases with a decreasing relative crest freeboard R_c/H_{m0} (Fig. 14) up to values of $b = 1.8$ for very low relative crest freeboards. These values are positioned in between the value of $b = 0.75$ for traditional sea defense structures and the values of b for negative crest freeboards (Hughes and Nadal, 2009) as suggested in Section 3. When the relative crest freeboard is larger (e.g. for traditional sea defence structures) only the largest waves overtop the crest of the structure. A decrease in relative crest freeboard results in overtopping of a larger percentage of the waves, including the medium-sized waves. Consequently, the probability distribution of the wave-by-wave overtopping volumes is more even distributed.

The different shape of the best Weibull fits of the individual overtopping volumes between small relative crest freeboards and large relative crest freeboards is illustrated by comparing Figs. 6 to 15. The data points in Fig. 15 correspond to a relative crest freeboard $R_c/H_{m0} = 1.04$ (with $\cot\alpha = 1.0$), while the relative crest freeboard in Fig. 6 is only 0.20 (with $\cot\alpha = 0.58$). The solid line of the best Weibull fit in Fig. 15 is positioned near the dash-dotted line corresponding to $b = 0.75$, as expected for the larger relative crest freeboard. The value of the shape factor is $b = 0.7$, which is much smaller than the value of 1.2 found for the example in Fig. 6.

The shape factors of the UG10 tests with non-Rayleigh distributed wave heights are larger than for the tests with Rayleigh distributed wave heights (Fig. 16). Nevertheless, a similar effect of the relative crest freeboard on the shape factor b is observed.

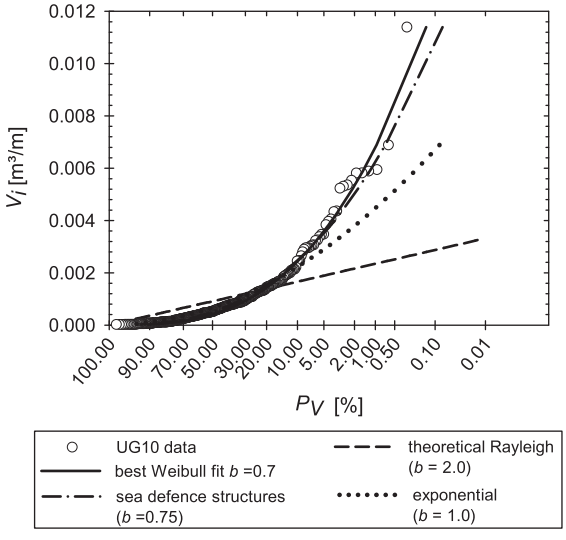

Fig. 15. Probability distribution of individual wave overtopping volumes for UG10 test results with $H_{m0} = 0.067$ m, $R_c = 0.07$ m, $T_p = 1.28$ s and $\cot\alpha = 0.58$. The corresponding relative crest freeboard is $R_c/H_{m0} = 1.04$.

5.5. Effect of wave steepness on shape factor b

When plotting the shape factor b as a function of the wave steepness $s_{m-1,0}$ [−] for test results of the UG10 dataset with $\cot\alpha = 1.0$ and $R_c = 0.045$ m and Rayleigh distributed wave heights (Fig. 17), no clear effect of the wave steepness on the shape factor of the Weibull distribution can be distinguished. Based on similar graphs for other sets of slope angle and crest freeboard, the general conclusion is drawn that the effect of the wave steepness on the shape of the Weibull distribution of the individual volumes for steep low-crested slopes is negligible compared to the effects of the slope angle (Section 5.3) and the relative crest freeboard (Section 5.4). This is in contrast to the findings by Besley (1999) that an increase in the

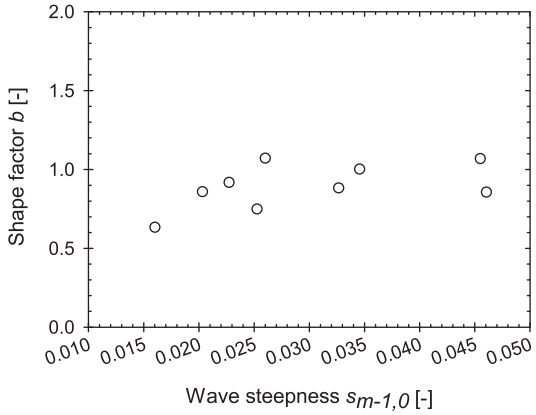

Fig. 17. Effect of the wave steepness on the shape factor b, for UG10 test results with $\cot\alpha = 1.0$ and $R_c = 0.045$ m—Rayleigh distributed wave heights.

value of the shape factor occurs for increasing wave steepness (Table 2). Note that the effect of the wave steepness on the shape of the Weibull distribution for rubble mound breakwaters has also been neglected (Bruce et al., 2009).

5.6. Prediction formula for shape factor b of Weibull distribution for steep low-crested slopes

Based on Sections 5.3 to 5.5, the shape factor b of the two-parameter Weibull distribution of the individual overtopping volumes for steep low-crested slopes appears to be a function of the slope angle and the relative crest freeboard. The effect of the wave steepness on b is negligible.

The shape factor b describes a decreasing exponential trend for increasing relative crest freeboard that is quasi-parallel for each value of the slope angle (Fig. 16). The exponential trend lines become horizontal for relatively large crest freeboards; the corresponding values of the shape factor decrease for increasing slope angle (Fig. 12). Accordingly, the following expression is valid for the shape factor b (f_1 and f_2 are random functions here):

$$\begin{cases} b = \exp\left(-C1\dfrac{R_c}{H_{m0}}\right) + C2 \\ C1 = f_1(\cot\alpha) \\ C2 = f_2(\cot\alpha) \end{cases} \quad (22)$$

Since the trend lines for each slope angle in Fig. 16 are quasi-parallel, the dependency of $C1$ on the slope angle is expected to be rather weak. Based on Section 5.3, f_2 is expected to be a linear function of cot α, increasing for an increasing value of cot α.

Values of $C1$ and $C2$ have been determined based on a non-linear regression analysis of the shape factors of the UG10 test results, for each category of the slope angle, containing both tests with Rayleigh and non-Rayleigh distributed wave heights. The corresponding values are given in Table 4 and visually shown in Figs. 18 and 19.

Table 4 confirms that the dependency of the coefficient $C1$ on the slope angle is relatively weak. It approximates the constant value of 2.0 (Fig. 18). Furthermore, the coefficient $C2$ increases linearly for increasing value of cot α (Fig. 19).

Eventually, the following prediction formula for the shape factor b for steep low-crested slopes has been found based on the UG10 test results:

$$b = \exp\left(-2.0\frac{R_c}{H_{m0}}\right) + (0.56 + 0.15\ \cot\alpha). \quad (23)$$

Measured and predicted values of the shape factor are shown in Fig. 20. The reliability of Eq. (23) is expressed by applying an *rmse* value of 0.10. Accordingly, the 90% prediction interval is determined by $b \pm 1.645\ rmse$; this interval is added to Fig. 20.

The shape factor corresponding to the horizontal part of the exponential function in Eq. (23) for cot $\alpha = 0.0$ and for relatively large crest freeboards equals 0.56. This value is closer to the value of 0.66 suggested by Besley (1999) for vertical walls under non-impulsive wave attack (Table 2) than to the value of 0.75 suggested by Franco et al. (1994) for vertical walls with a large relative crest freeboard in relatively deep water.

Table 4
Values of $C1$ and $C2$ (Eq. (22)) for UG10 test results.

cot α	$C1$	$C2$
2.75	1.92	0.93
2.14	2.07	0.91
1.73	1.90	0.83
1.43	1.79	0.76
1.19	1.97	0.71
1.00	2.55	0.75
0.84	2.64	0.74
0.58	1.90	0.60
0.36	1.91	0.59

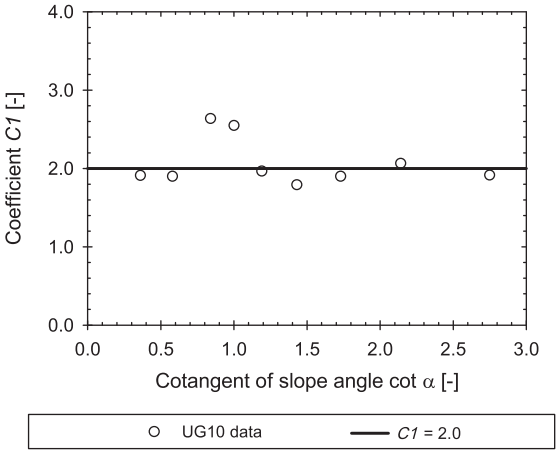

Fig. 18. Effect of slope angle on the coefficient $C1$ of Eq. (23).

The validity of Eq. (23) is confirmed when plotting experimentally determined shape factors and predicted values of Eq. (23) as a function of the relative crest freeboard for cot $\alpha = 2.75$ (Fig. 21) and cot $\alpha = 0.36$ (Fig. 22).

Since the coefficients $C1$ and $C2$ are based on all UG10 test results, the effect of the distribution of the wave heights (Rayleigh or non-Rayleigh) is included in the scatter of the shape factor of the Weibull distribution for the individual overtopping volumes of steep low-crested slopes.

The shape of the Weibull distribution of the individual overtopping volumes for steep low-crested structures is determined based on Eq. (23). In order to determine the scale factor a (Eq. (2)), knowledge on the probability of overtopping P_{ow} of steep low-crested slopes is required. This is the subject of the next Section 6.

6. Overtopping probability for smooth impermeable steep slopes with low crest freeboards

The expressions for the probability of overtopping P_{ow} in Section 2.2 are based on a Rayleigh distribution of the run up heights, requiring the wave heights to be Rayleigh distributed as well. It is unclear if the run-up heights are Rayleigh distributed when the wave heights are not Rayleigh distributed. Since the structures studied in this paper feature relatively low crest freeboards, the effect

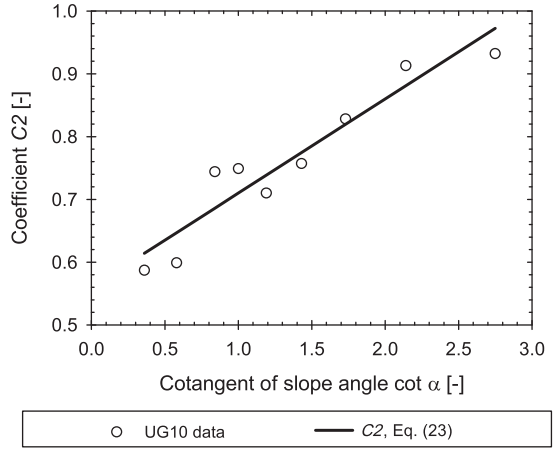

Fig. 19. Effect of slope angle on the coefficient $C2$ of Eq. (23).

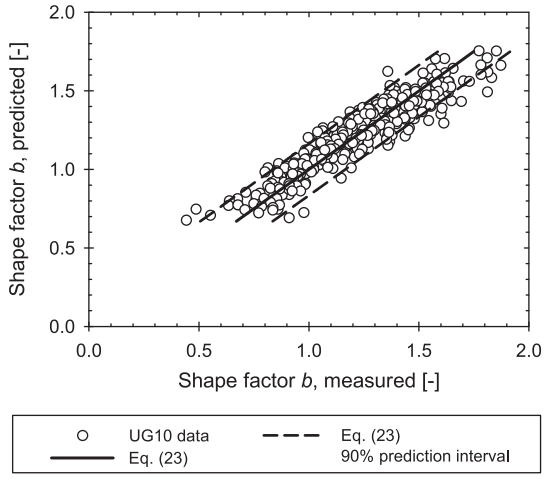

Fig. 20. Comparison between measured and predicted (Eq. (23)) shape factors.

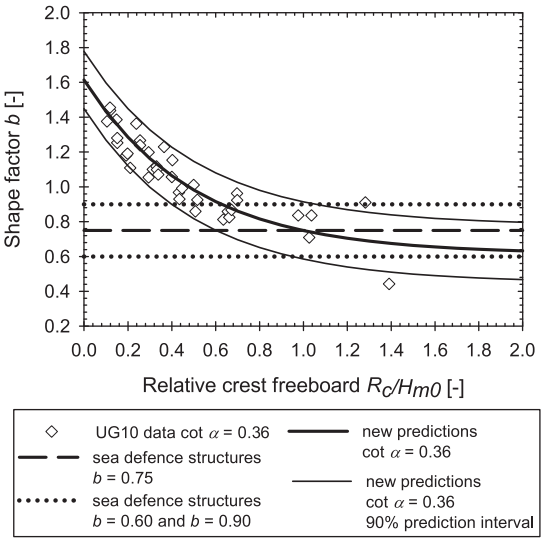

Fig. 22. Effect of the relative crest freeboard on the shape factor b (measured and predicted by Eq. (23)) for UG10 test results with cot $\alpha = 0.36$.

of non-Rayleigh distributed wave heights on P_{ow} is expected to be relatively small.

The effects of the slope angle, relative crest freeboard and wave steepness on the probability of overtopping for the UG10 test results are discussed in the following three Sections 6.1 to 6.3.

6.1. Effect of slope angle on P_{ow}

Translating the relative 2% run-up height in Fig. 3 to probabilities of overtopping using Eqs. (10) and (11) results in Fig. 23, to which specific measured values of P_{ow} for the UG10 dataset are added for a given relative crest height of R_c/H_{m0} 0.45. The effect of the slope angle on the probability of overtopping is clearly visible. A significant decrease in P_{ow} occurs for increasing slope angle from the values predicted by Eqs. (12a)–(12b) and Eqs. (14a)–(14b) toward the theoretical value for vertical walls. This trend also occurs for tests of the UG10 test series with non-Rayleigh distributed wave heights (Fig. 24).

Based on Fig. 23, it is clear that when the breaker parameter increases due to a decrease in the wave steepness (heavily breaking waves on very depth-limited foreshores, see Van Gent, 2001), an increase in the probability of overtopping occurs. On the other hand, when an increase in breaker parameter occurs due to an increase in the slope angle, a decrease in the probability of overtopping is to be expected. When the slope becomes steeper, more energy is lost through wave reflection. Hence, a smaller percentage of the waves is able to run up the slope and to overtop the crest of the structure.

The value of P_{ow} for vertical walls is related to the theoretical value of the relative 2% run-up height given in Eq. (17). Based on Eqs. (10) and (11), the corresponding expression for the probability of overtopping for vertical walls is found:

$$\chi = 0.51 \cdot 1.4 = 0.71 \tag{24a}$$

$$\Rightarrow P_{ow} = \exp\left(-\left(1.4\frac{R_c}{H_{m0}}\right)^2\right). \tag{24b}$$

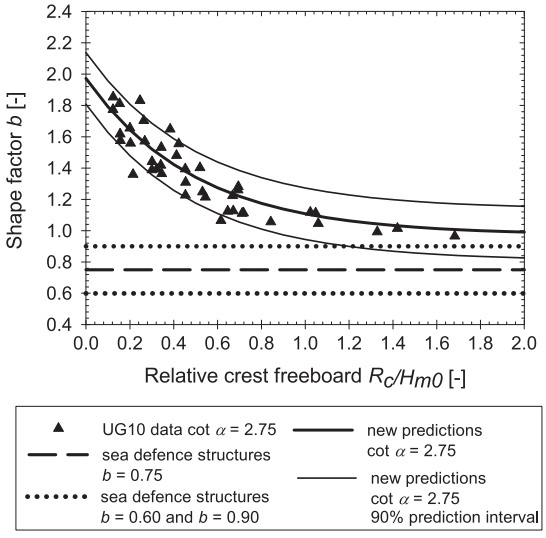

Fig. 21. Effect of the relative crest freeboard on the shape factor b (measured and predicted by Eq. (23)) for UG10 test results with cot $\alpha = 2.75$.

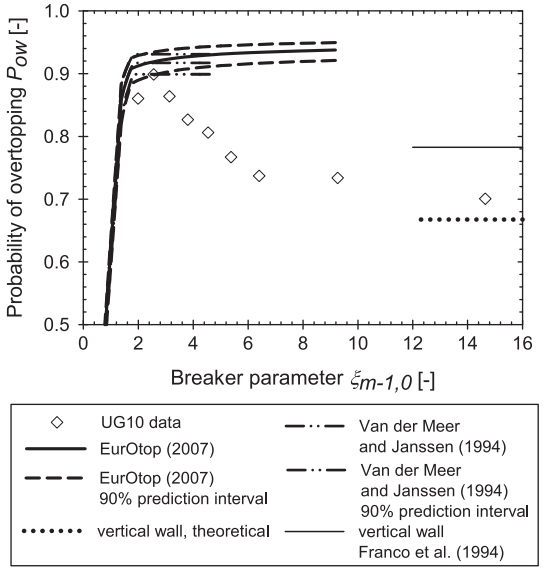

Fig. 23. Measured and predicted probabilities of overtopping for UG10 test results with $H_{m0} = 0.100$ m, $R_c = 0.045$ m and $T_p = 1.534$ s versus the breaker parameter—Rayleigh distributed wave heights.

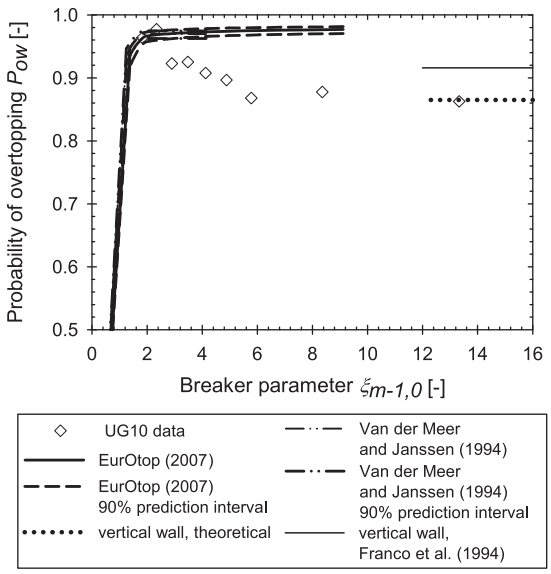

Fig. 24. Measured and predicted probabilities of overtopping for UG10 test results with $H_{m0}=0.167$ m, $R_c=0.045$ m and $T_p=1.789$ s versus the breaker parameter—non-Rayleigh distributed.

Note that Franco et al. (1994) found a value of $\chi=0.91$ for vertical walls in relatively deep water, resulting in a probability of overtopping that is larger than calculated by Eq. (24b):

$$P_{ow} = \exp\left(-\left(1.1\frac{R_c}{H_{m0}}\right)^2\right). \tag{24c}$$

Eqs. (24b) and (24c) show that the probability of overtopping is according to a Rayleigh distribution. The effect of the relative crest freeboard on P_{ow} is studied in Section 6.2.

6.2. Effect of relative crest freeboard on P_{ow}

A decrease in the relative crest freeboard R_c/H_{m0} causes an increase in P_{ow} for a specific slope angle (Fig. 25). This is valid for all UG10 tests, with both Rayleigh and non-Rayleigh distributed wave heights (Fig. 26). The probabilities of overtopping for tests of the

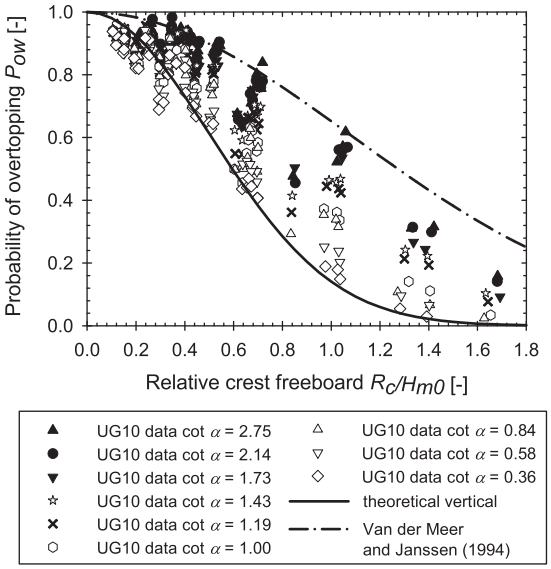

Fig. 25. Effect of relative crest freeboard on probability of overtopping for UG10 test results, categorized by the slope angle.

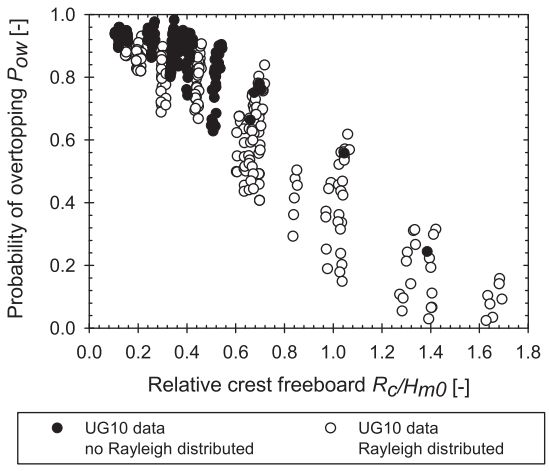

Fig. 26. Effect of relative crest freeboard on probability of overtopping for UG10 test results—Rayleigh distributed versus non-Rayleigh distributed wave heights.

UG10 test series with non-Rayleigh distributed wave heights are positioned among the values of P_{ow} for the tests with Rayleigh distributed wave heights. This confirms that the effect of the wave height distribution is small for relatively small crest freeboards.

There are two physical bounds for P_{ow} that are clearly visible in Figs. 25 and 26: P_{ow} becomes 1.0 for a zero relative crest freeboard (all waves overtop the crest of the structure) and 0.0 for very large relative crest freeboards (no waves overtop the structure), the last dependent of the slope angle.

The predicted effect of the relative crest freeboard on the probability of overtopping is shown in Fig. 25 for the theoretical value of P_{ow} for vertical walls (Eqs. (24b) and (24c)) and for the probability of overtopping related to the relative 2% run-up height predicted by Van der Meer and Janssen (1994) (Eqs. (25a)–(25b)). The UG10 data points are largely positioned in between the prediction lines corresponding to Eqs. (24b) and (25b).

$$\chi = 0.51\cdot 3.0 = 1.53 \tag{25a}$$

$$\Rightarrow P_{ow} = \exp\left(-\left(0.65\frac{R_c}{H_{m0}}\right)^2\right). \tag{25b}$$

6.3. Effect of wave steepness on P_{ow}

The effect of the wave steepness $s_{m-1,0}$ on the probability of overtopping P_{ow} is shown in Fig. 27 for the tests of the UG10 dataset with

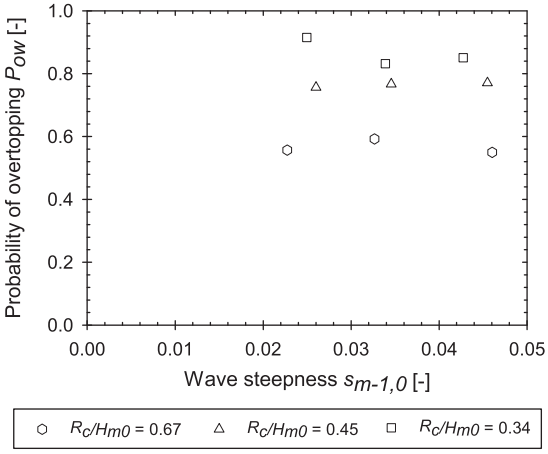

Fig. 27. Effect of wave steepness on probability of overtopping for UG10 test results with cot $\alpha=1.0$, $R_c=0.045$ m and $H_{m0}=0.067$ m, 0.100 m and 0.133 m. Data categorized by the wave height.

cot α = 1.0, R_c = 0.045 m and H_{m0} = 0.067 m, 0.100 m and 0.133 m. The data points are categorized by the wave height. Based on Fig. 27, the effect of the wave period on P_{ow} is considered to be negligible compared to the effects of the slope angle (Section 6.1) and the relative crest freeboard (Section 6.2). Similar graphs for other sets of cot α= and R_c/H_{m0} confirm this conclusion.

6.4. Prediction formula for probability of overtopping P_{ow} for steep low-crested slopes

Based on Fig. 25, the increase in P_{ow} with a decrease in relative crest freeboard R_c/H_{m0} for a particular slope angle is assumed to be well described by a Rayleigh distribution using the relative crest freeboard:

$$P_{ow} = \exp\left(-\left(C3\frac{R_c}{H_{m0}}\right)^2\right). \quad (26)$$

The expression in Eq. (26) is similar to Eq. (10), with $\chi = 1/C3$. It takes into account the two physical bounds given in Section 6.2. Due to the negligible effect of the wave steepness on the probability of overtopping, $C3$ [−] is not a function of the wave steepness. Since Eq. (26) contains the relative crest freeboard, $C3$ is expected to be only a function of the slope angle. Indeed the values of P_{ow} of the UG10 test results are accurately described by a Rayleigh distribution for each category of the slope angle. However, when plotting the values of $C3$ obtained by $C3 = \sqrt{-(\ln(P_{ow}))}/(R_c/H_{m0})$ against the relative crest freeboard (Fig. 28), one may conclude that $C3$ is still a function of the relative crest freeboard. The values of $C3$ are approximately independent of the relative crest freeboard for $R_c/H_{m0} > 0.4$, but increase considerably when the relative crest freeboard decreases to very low values.

On the other hand, the probability of overtopping P_{ow} is expected to be approximately equal to 1.0 for very small relative crest freeboards. This means that the large values of $C3$ in Fig. 28 are introduced by the small relative crest freeboards R_c/H_{m0} in the expression $C3 = \sqrt{-(\ln(P_{ow}))}/(R_c/H_{m0})$.

Hence, the coefficient $C3$ is assumed to be independent of the relative crest freeboard, determined by the values of $C3$ with $R_c/H_{m0} > 0.4$ (Fig. 28).

The corresponding values of $C3$ are given in Table 5 for each value of the slope angle and shown in Fig. 29. These values are valid for tests both with and without Rayleigh distributed wave heights (part of the scatter).

Table 5
Values of $C3$ for UG10 test results.

cot α	$C3$
2.75	0.79
2.14	0.80
1.73	0.86
1.43	0.96
1.19	0.96
1.00	1.08
0.84	1.16
0.58	1.20
0.36	1.34

Based on Fig. 29, the values of $C3$ appear to be accurately described by a linear function of the cotangent of the slope angle (Eq. (27)). The reliability of Eq. (27) is expressed by applying an *rmse* value of 0.13 ($R_c/H_{m0} > 0.4$). The corresponding 90% prediction interval is added to Fig. 29.

$$C3 = 1.4 - 0.30\cot\alpha \quad (C3 > 0.65). \quad (27)$$

Note that Eq. (27) takes the theoretical value of 1.4 for vertical walls (Eq. (24b)) (cot α = 0.0). Furthermore, Eq. (27) approximately becomes equal to 0.65 (i.e. the value of $C3$ for milder slopes with non-breaking waves predicted by Van der Meer and Janssen (1994) (Eq. (25b))) for cot α = 2.5. For slopes milder than that value, P_{ow} should be predicted based on the existing formulations for P_{ow} of Van der Meer and Janssen (1994). Accordingly, the restriction $C3 > 0.65$ is added to Eq. (27).

The corresponding expression for the probability of overtopping is:

$$P_{ow} = \exp\left[-\left((1.4 - 0.30\cot\alpha)\frac{R_c}{H_{m0}}\right)^2\right]. \quad (28)$$

The *rmse* value based on the measured and predicted values of P_{ow} equals only 0.073, which shows that the predictions agree well with the measurements. This is also illustrated by the two graphs below (Figs. 30 and 31). Fig. 30 is similar to Fig. 21 (relative crest freeboard R_c/H_{m0} = 0.45) to which the predicted values by Eq. (28) (together with its 90% prediction interval) have been added. Fig. 31 shows a similar graph for a larger relative crest freeboard: R_c/H_{m0} = 1.04.

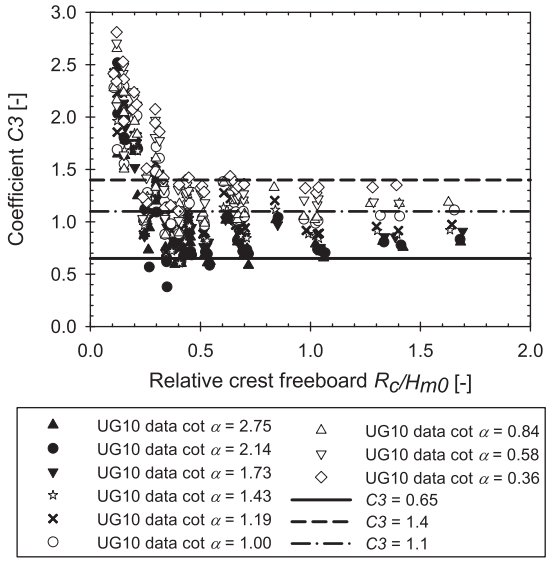

Fig. 28. Effect of the relative crest freeboard on the coefficient $C3$ of Eq. (27).

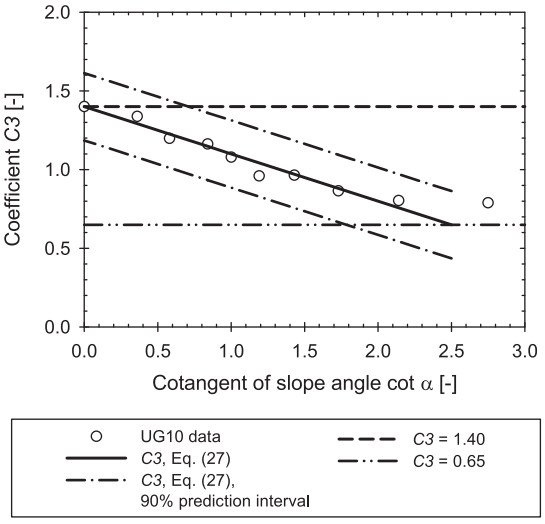

Fig. 29. Effect of the slope angle on the coefficient $C3$ of Eq. (27).

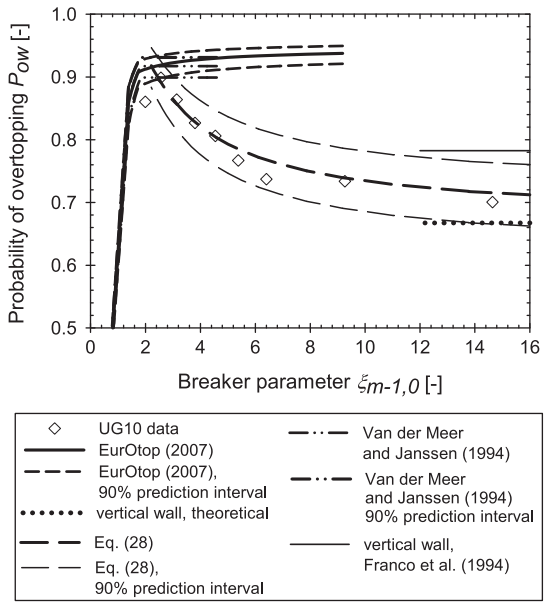

Fig. 30. Measured and predicted probabilities of overtopping for UG10 test results with $H_{m0}=0.100$ m, $T_p=1.534$ s and $R_c=0.045$ m versus the breaker parameter.

In both figures, the predicted probabilities of overtopping of Eq. (28) approach the data points of the UG10 test results quite accurately. Furthermore, the predictions tend toward the theoretical probability of overtopping for very large values of the breaker parameter (i.e. the asymptotic case of a vertical wall) and intersect the prediction line by Van der Meer and Janssen (1994) approximately at $\xi_{m-1,0}=3.0$. Both figures illustrate the validity of Eq. (28) within the ranges of application of the UG10 test series.

6.5. Prediction formula for relative 2% run-up height $R_{u2\%}/H_{m0}$ for steep low-crested slopes

Based on the expression for $C3$ in Eq. (27), Eq. (11) and taking into account $\chi=1/C3$, the following expression for the relative 2% run-up height has been derived for steep low-crested slopes in relatively deep water:

$$\frac{R_{u2\%}}{H_{m0}}=\frac{1}{0.71-0.15\cot\alpha}. \tag{29}$$

It is important to note that the relationship between $R_{u2\%}/H_{m0}$ and P_{ow} established by Eqs. (10) and (11) is based on knowledge concerning $R_{u2\%}/H_{m0}$ (non-overtopped structures) applied to structures with a limited amount of wave overtopping (Franco et al., 1994; Van der Meer and Janssen, 1994). This means that deriving an expression for $R_{u2\%}/H_{m0}$ based on measurements of $\cot\alpha$ is only valid for sloped structures with relatively large crest freeboards. When the relative crest freeboards are smaller, the expression derived for $R_{u2\%}/H_{m0}$ is only approximate. Since the UG10 test results feature steep low-crested slopes, the expression for the relative 2% run-up height in Eq. (29) only approximates the values of $R_{u2\%}/H_{m0}$ for steep slopes in relatively deep water. Due to the fact that the coefficients $C3$ (Section 6.4) are determined for the UG10 test results with $R_c/H_{m0}>0.4$ that are only slightly dependent of the relative crest freeboard (Fig. 28), the deviations between the real values of $R_{u2\%}/H_{m0}$ for steep slopes in relatively deep water and their predictions by Eq. (29) are expected to be relatively small.

A figure similar to Fig. 3 is shown in Fig. 32, to which the predictions by Eq. (29) have been added. The new prediction formula clearly confirms the expected decreasing trend of the relative 2% run-up heights for steeper slopes with increasing slope angle in relatively deep water (Section 3.3).

7. Conclusions

The probability distribution of the individual overtopping volumes of steep low-crested slopes has been investigated based on the UG10 test results and through a comparison with existing formulations from literature.

Similar to traditional sea defense structures, the individual overtopping volumes appear to follow a two-parameter Weibull probability distribution, characterized by a scale factor a and a shape factor b. The scale factor a of the Weibull distribution is closely related to the probability of overtopping P_{ow}, which has also been studied based on the UG10 test results.

Both the shape factor b and the probability of overtopping P_{ow} appear to depend on the slope angle and relative crest freeboard. The effect of the wave steepness is negligible.

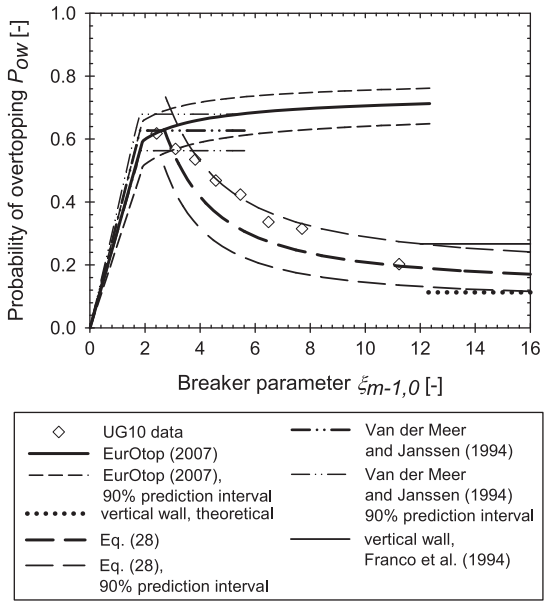

Fig. 31. Measured and predicted probabilities of overtopping for UG10 test results with $H_{m0}=0.067$ m, $T_p=1.534$ s and $R_c=0.070$ m versus the breaker parameter.

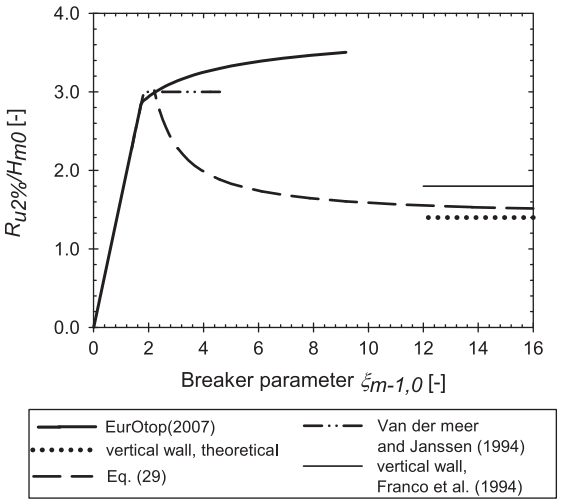

Fig. 32. Predicted relative 2% run-up heights with $H_{m0}=0.100$ m, $T_p=1.534$ s and $R_c=0.045$ m versus the breaker parameter.

The effect of the relative crest freeboard on the shape factor of the Weibull distribution is described by a negative exponential function. When $R_c/H_{m0}<1.2$, values of the shape factor $b>0.75$ (typical value for traditional sea defense structures) have been found for the UG10 test results (up to $b=1.5$), both for milder and steeper slopes. Accordingly, a smaller maximum volume V_{max} and a larger percentage of medium-sized overtopping volumes occur for low-crested structures compared to structures with a relatively large crest freeboard. This means that the design of traditional structures with small relative crest freeboards is conservative when applying the value of the shape factor for traditional sea defense structures $b=0.75$. Furthermore, b follows a linear increasing trend for a decreasing slope angle, even for relatively large crest freeboards. A prediction formula (Eq. (23)) has been derived based on the UG10 test results, which takes into account these effects.

The values of the overtopping probability P_{ow} determined for the UG10 test results with steep slopes appear to be overpredicted by the commonly used empirical prediction formulae from literature. This is due to the fact that the existing prediction formulae of P_{ow} for larger breaker parameters are based on tests with small values of the wave steepness induced by heavily breaking waves on very depth limited situations. For deeper water and $\xi_{m-1,0}\approx 3.0$, P_{ow} is more or less constant. When larger breaker parameters of $\xi_{m-1,0}>\approx 3.0$ are caused by larger slope angles, a decrease in probability of overtopping occurs which is described by a linear function of the cotangent of the slope angle. Furthermore, the effect of the relative crest freeboard on P_{ow} is described by a Rayleigh distribution of R_c/H_{m0}, decreasing from $P_{ow}=1.0$ for a zero crest freeboard (all waves overtop the structure) to $P_{ow}=0.0$ for large relative crest freeboards (no waves overtop the structure). Similar to b, a prediction formula has been derived that takes into account these effects.

Based on this prediction formula and the relationship between the relative 2% run-up height $R_{u2\%}/H_{m0}$ and P_{ow} established in literature for sloped structures with limited wave overtopping, a new prediction formula has been proposed for $R_{u2\%}/H_{m0}$ at steep slopes in relatively deep water. Since this formula is based on the UG10 test results that feature relatively small crest freeboards, the new predictions of $R_{u2\%}/H_{m0}$ are only approximate. Nevertheless, these predictions indicate that a decrease in the relative 2% run-up height should occur for steep slopes in relatively deep water with increasing slope angle.

The importance of the distribution of the incident wave heights has been investigated, both for the shape factor b and for the probability of overtopping P_{ow}. When the wave heights are not Rayleigh distributed, slightly larger values of the shape factor are found, while the effect of the wave height distribution on the probability of overtopping appears to be relatively small. The effect of the distribution of the wave heights is part of the scatter on the new prediction formulae for b and P_{ow} based on the UG10 test results.

The improved knowledge on the probability distribution of low-crested structures achieved in this paper allows to carry out more realistic simulations of wave-by-wave overtopping volumes in order to optimize the design of the reservoir and the turbine control strategy of OWECs.

Moreover, this knowledge is applicable to sea defense structures in severe storm conditions, when a low crest freeboard occurs. Applying a shape factor $b>0.75$ results in more realistic (lower) maximum overtopping volumes than when applying the shape factor $b=0.75$ for traditional sea defense structures with relatively large crest freeboards.

Acknowledgments

The research is funded by a Ph.D. grant from the Fund for Scientific Research Flanders (FWO – Vlaanderen), Belgium. We sincerely thank the technicians at Ghent University (Belgium), for their help with constructing the test set-up. Jan Goormachtigh and Walid Harchay are strongly acknowledged for assisting in the experiments leading to the UG10 dataset.

References

Battjes, J.A., Groenendijk, H.W., 2000. Wave height distributions on shallow foreshores. Coastal Engineering 40 (3), 161–182.
Besley, P., 1999. Overtopping of Seawalls—Design and Assessment Manual, R&D Technical Report W178. Environment Agency, Bristol, UK.
Besley, P., Stewart, T., Allsop, N.W.H., 1998. Overtopping of vertical structures: new prediction methods to account for shallow water conditions. Proc. Coastlines, Structures and Breakwaters, London, UK, pp. 46–57.
Bruce, T., van der Meer, J.W., Franco, L., Pearson, J.M., 2009. Overtopping performance of different armour units for rubble mound breakwaters. Coastal Engineering 56 (2), 166–179.
EurOtop, 2007. EurOtop. Wave Overtopping of Sea Defences and Related Structures: Assessment Manual, Environment Agency, UK/ENW Expertise Netwerk Waterkeren, NL/KFKI Kuratorium für Forschung im Küsteningenieurwesen, DE.Pullen, T., Allsop, N.W.H., Bruce, T., Kortenhaus, A., Schüttrumpf, H., van der Meer, J.W., . http://www.overtopping-manual.com.
Franco, L., de Gerloni, M., van der Meer, J., 1994. Wave overtopping on vertical and composite breakwaters. Proc. 24th International Conference on Coastal Engineering. ASCE, New York, pp. 1030–1044.
Hughes, S.A., Nadal, N.C., 2009. Laboratory study of combined wave overtopping and storm surge overflow of a levee. Coastal Engineering 56 (3), 244–259.
Kofoed, J.P., 2002. *wave overtopping of marine structures—utilization of wave energy*. PhD Thesis, Aalborg University, Aalborg, DK.
Schüttrumpf, H., 2001. Wellenüberlaufströmung bei Seedeichen - Experimentelle und theoretische Untersuchungen. Phd Thesis, Technischen Universität Carolo-Wilhelmina, Braunschweig, DE.
TAW, 2002. Technical Report Wave Run-up and Wave Overtopping at Dikes, Technische Adviescommissie voor de Waterkeringen, Delft.
Van der Meer, J.W., Janssen, J.P.F.M., 1994. Wave run-up and wave overtopping at dikes and revetments. Delft Hydraulics.
Van Gent, M.R.A., 2001. Wave runup on dikes with shallow foreshores. Journal of Waterway Port Coastal and Ocean Engineering-Asce 127 (5), 254–262.

Glossary

a: scale factor of Weibull distribution [m³/m]
b: shape factor of Weibull distribution [−]
a': $1/\Gamma(1+1/b)$ [−]
$C1, C2$: coefficients Eq. (22), prediction formula b [−]
$C3$: coefficient Eq. (26), prediction formula P_{ow} [−]
g: acceleration due to gravity [m/s²]
H_s: significant wave height [m]
H_{m0}: spectral wave height of the incident waves at the toe of the structure [m]
m_{-1}: first negative moment of the incident wave spectrum [m²s]
m_0: zeroth moment of the incident wave spectrum [m²]
N_{ow}: number of overtopping waves [−]
N_w: number of incident waves [−]
OWECs: Overtopping Wave Energy Converters
q: average overtopping rate [m³/s/m]
rmse: root-mean-square error [−]
P_{ow}: probability of overtopping [−], defined by N_{ow}/N_w
P_V: exceedance probability of overtopping volume V [−]
R_c: crest freeboard, i.e. the vertical distance between the crest of the structure and the still water level [m]
$R_{u2\%}$: 2% run-up height [m]
s_p: wave steepness defined by $s_p=2\ \pi\ H_s/(g\ T_p^2)$ [−]
$s_{m-1,0}$: wave steepness defined by $s_{m-1,0}=2\ \pi\ H_{m0}/(g\ T_{m-1,0}^2)$ [−]
T_0: sum of the wave periods of each wave in the wave train [s]
T_i: wave period of individual wave in wave train [s]
T_m: mean wave period [s]
$T_{m-1,0}$: spectral incident wave period at the toe of the structure defined by $T_{m-1,0}=m_{-1}/m_0$ [s]
T_p: peak incident wave period [s]
v_0: total overtopping volume [m³/m]
v_i: individual overtopping volume [m³/m]
v_{max}: maximum individual overtopping volume [m³/m]
$\bar{V}_{meas}$: measured mean overtopping volume [m³/m]
$\bar{V}_{theor}$: theoretical mean overtopping volume [m³/m]
α: slope angle of the structure [rad]
χ: Coefficient relating P_{ow} to R_c/H_{m0} (Eq. (10)) [−]
Γ: mathematical gamma function
μ: mean value of parameter
σ: standard deviation [−]
$\xi_{m-1,0}$: breaker parameter, defined by $\xi_{m-1,0}=\tan\alpha/\sqrt{s_{m-1,0}}$ [−]
ξ_p: breaker parameter, defined by $\xi_p=\tan\alpha/\sqrt{s_p}$ [−]